

Gas holdup in tapered bubble column using pseudoplastic non-Newtonian liquids

Sumit Kumar Jana[‡], Asit Baran Biswas, and Sudip Kumar Das[†]

Department of Chemical Engineering, University of Calcutta, 92, A. P. C. Road, Kolkata-700 009, India
(Received 3 August 2013 • accepted 7 October 2013)

Abstract—Experimental studies on the gas holdup in two tapered bubble columns using non-Newtonian pseudoplastic liquid have been reported. The effects of different variables such as gas flow rate, liquid viscosity, bed height, and orifice diameter of sieve plate on gas holdup have been investigated. An empirical correlation has been developed for the prediction of the gas holdup as a function of various measurable parameters of the system. The correlation is statistically acceptable.

Keywords: Bubble Columns, Non-Newtonian Liquid, Pseudoplastic Liquid, Gas Hold-up

INTRODUCTION

Bubble columns are used as absorbers, strippers, reactors and fermenters in chemical process industries. A bubble column has no moving parts, simple construction, good mixing and good heat and mass transfer capacity, temperature control; minimum maintenance and low capital cost make it most advantageous. It has some disadvantages also: bubble coalescence, high pressure drop, considerable back mixing in both phases, short residence time of gas and complex hydrodynamics flow patterns. Biotechnology, food processing and pharmaceutical processes frequently use bubble columns and often use them to process highly viscous liquids. Design and scale up of bubble columns are difficult tasks because the interaction of gas-liquid, shear at the interface and the wall, and the hydrodynamics are not fully understood. The hydrodynamics parameters of a bubble column depend on the operating conditions, geometry and physiochemical properties of the phases and the gas distributor system [1-4].

Deckwer [5] and Kantarci et al. [6] have outlined a design procedure of a bubble column reactor. Various types of bubble columns and their modifications are described by Shah et al. [7]. Modified bubble columns include loop reactors, horizontal sparger bubble column, downflow bubble column, sectionalized bubble column which are reported in the literature [8-11]. Down flow bubble columns with ejector type gas distributor are reported by Kundu et al. [12] and Mandal et al. [13]. Taper columns and bubble columns have also been used in industrial practice in fluidization, segregation of particles in fluidized columns, flotation cells, biochemical reactions, biological wastewater treatment, etc. for more than few decades [14-27]. Zhang et al. [18] reported that the gas holdup in a cylindrical bubble column does not change in the axial direction at low gas velocity but decreases slightly at high gas velocity from the bottom to top, whereas in a tapered bubble column the axial gas holdup

decreases from bottom to the top [20]. Here bubbles are rising from the bottom as a spherical shape and then coalescing to bigger bubbles; their shape changes from circular to flatter and rupture to small bubbles [19,20]. The flow pattern in the tapered bubble column consists of two zones, central zone and annular region. In the central zone most of the bubbles rise, whereas bubble breakup and downward flow occur in the annular region [21].

In the biotechnology, chemical, petrochemical, polymer and pharmaceutical industries the liquids used are often non-Newtonian. In fermentation, initially the liquid is Newtonian and then gradually it is converted to non-Newtonian [28]. Bubbles in non-Newtonian liquid behave as various shapes and under the action of surface tension, inertial force, viscous drag force and buoyancy, together with the complex rheological behavior of the liquids. Hence the bubble flows in these liquids have different characteristics than that of Newtonian liquids [29]. Only few literatures are available using non-Newtonian liquid in a bubble column [28-37]. Chandrakar [33] reported detailed experimental studies on gas-non-Newtonian liquid upflow bubble column with ejector type gas distributor. Lakota [36] studied the upflow bubble column using non-Newtonian liquids with concurrent upflow mode, and also liquid batch mode and developed an empirical correlation for holdup prediction for each case. Pradhan et al. [37] studied the effects of internals in the bubble column using non-Newtonian pseudoplastic liquids. Das et al. [38] developed an empirical correlation for the prediction of holdup for gas-non-Newtonian liquid upflow in a vertical column. Mandal et al. [39] studied gas entrainment and holdup characteristics in a downflow bubble column with both Newtonian and non-Newtonian liquids and later they also reported the frictional pressure drop [13]. Chandarkar et al. [40] reported that the gas dispersion in non-Newtonian liquid in a co-current vertically upflow bubble column. Liquid circulation induced by the bubble movement is an important phenomenon observed in gas bubbling in viscous liquids and is reviewed by Haque et al. [41]. Anastasiou et al. [42] developed an empirical correlation to predict the gas holdup for shear thinning non-Newtonian liquid in bubble columns with a metal porous sparger to provide very fine air bubbles. In the present study taper bubble columns are fabricated to study their hydrodynamic characteristics using non-Newtonian pseudoplastic liquids.

[†]To whom correspondence should be addressed.
E-mail: drsudipkdas@vsnl.net

[‡]Present address: Department of Chemical and Polymer Engineering, Birla Institute of Technology, Mesra-835215, Ranchi, India
Copyright by The Korean Institute of Chemical Engineers.

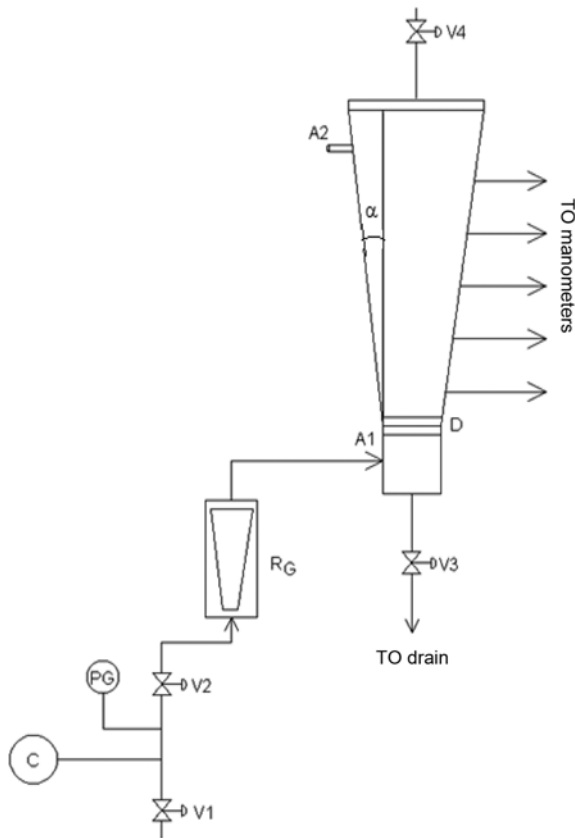


Fig. 1. Schematic diagram of experimental setup.

A1: Air inlet; A2: Air outlet; Manometers; D: Distributor; C: Compressor; PG: pressure Gauge; R_G : Rotameter for gas; V1-V4: Control valves, α : taper angle

EXPERIMENTAL DETAILS

A schematic diagram of the experimental setup is shown in Fig. 1.

It consists of a tapered bubble column, manometers for pressure measurement, distributor plate (D) to distribute the air, compressor (C), pressure gauge (PG), rotameter (R_G) for flow measures and other accessories.

The tapered bubble columns were made of thick Perspex and square shaped. A perforated plate made of Perspex of different hole diameters was used for air distribution and connected to the columns by means of flanges. Air inlet was provided in columns by means of nozzles of 4 mm diameter and then distributed through the distributor in the columns and entered into the columns. The distributor was a perforated Perspex plate. Three different plates of different hole diameters were used as distributor. Two tapered bubble columns of different cross-section areas were used for the experiment. Detailed dimensions of the columns are shown in Table 1. Columns were fitted to vertically by means of clamps to avoid any vibration.

The dilute solutions of sodium salt of carboxymethyl cellulose (SCMC) were used as non-Newtonian pseudoplastic liquids. The non-Newtonian liquid was prepared by taking desired amount of SCMC, dissolved in tap water; a few drops of formaldehyde were added to avoid biological degradation and kept around one night for aging. Four different SCMC concentrations, 0.2–0.8 kg/m³, were used for the experiment. The dilute solution of SCMC is a time independent pseudoplastic fluid and its rheology is described by Oswald de-Waele or Power law model [36,37],

$$\tau = K \left(-\frac{dV}{dr} \right)^n \quad (1)$$

where, K and n are the constants for the particular liquid with $n < 1$. The constant K is the consistency index of the liquid and the higher the value of K the more viscous is the fluid. The rheological properties of the SCMC solutions were measured by means of pipeline viscometer. DuNouy tensiometer and a specific gravity bottle measured surface tension and density, respectively. The physical properties of the liquid are shown in Table 2.

Table 1. Dimension of the bubble columns

Characteristic parameters	Larger tapered bubble column	Smaller tapered bubble column
	TB2	TB1
Thickness of Perspex sheet, m	0.0127	0.0127
Height of column, m	1.83	1.83
Top plate area, m ²	0.1016 × 0.1016	0.0762 × 0.0762
Bottom plate area, m ²	0.0508 × 0.0508	0.0508 × 0.0508
Equivalent diameter, m	0.0692 ≤ D_c ≤ 0.0710	0.0605 ≤ D_c ≤ 0.0614
Taper angle (deg)	0.86	0.44
Orifice diameter of different sieve plates used, m	0.00277, 0.00357, 0.00436	0.00277, 0.00357, 0.00436
Number of orifice in the sieve plate	50	50
Pitch	square	square
Distance from the air distributor		
Taping no.1, m	0.0508	0.0508
Taping no.2, m	0.2032	0.2032
Taping no.3, m	0.3556	0.3556
Taping no.4, m	0.5080	0.5080
Taping no.5, m	0.6604	0.6604
Taping no.6, m	0.8128	0.8128

Table 2. Physical properties of the SCMC solutions

Concentration Kg/m ³	Flow behavior index (n)	Consistency index K (Ns ⁿ /m ²)	Density ρ (Kg/m ³)	Surface tension σ (N/m)
0.2	0.9013	0.0138	1001.69	0.07834
0.4	0.7443	0.1149	1002.13	0.08003
0.6	0.6605	0.3154	1002.87	0.08142
0.8	0.6015	0.6486	1003.83	0.08320

The liquid heights used for the experiments were 1.12 m, 1.17 m and 1.22 m for both columns. The air at a pressure 1 kg/cm² gauge was introduced into the columns, and under steady state condition, readings of manometers attached to the tapings were noted, and also the height of liquid column was noted. Manometers were attached to the tapings as shown in Fig. 1, which were located at different heights in the column. From the manometer readings pressure drop was determined. The experiments were repeated several times to ensure the reproducibility of the data. The air flow rate used for the experiment varied from 5.8×10^{-6} to 4.61×10^{-4} m³/s. The temperature was maintained at atmospheric temperature 30 ± 2 °C.

The gas holdup for a particular gas flow rate is the fraction of the total gas-liquid volume that is occupied by the gas. This gas holdup is measured experimentally by using the following expression:

$$\varepsilon_g = \frac{V - V_o}{V} \quad (2)$$

RESULTS AND DISCUSSION

1. Effective Shear Rate

In the case of non-Newtonian liquids the viscosity is a function of shear rate and it is generally expressed as effective viscosity, μ_{eff} . To estimate the effective viscosity, the effective shear rate, $\dot{\gamma}_{eff}$, in the bubble column has to be calculated first. For the Power law model the effective viscosity is defined as

$$\mu_{eff} = K \dot{\gamma}_{eff}^{n-1} \quad (3)$$

Literature review suggested that $\dot{\gamma}_{eff}$ is proportional to the superficial gas velocity as the shear originates from the relative velocity between bubbles and the liquid in the bubble column and expressed as [31,43,44],

$$\dot{\gamma}_{eff} = C u_g \quad (4)$$

The constant, C, value suggested by different researchers is as follows:

Nishikawa et al. [43]	C=5,000 m ⁻¹ for n varies from 0.72 to 1
Henzler [44]	C=1,500 m ⁻¹ for n varies from 0.38 to 0.82
Schumpe and Deckwer [31]	C=2,800 m ⁻¹ for n varies from 0.180 to 1

Nishikawa et al. [43] obtained the value of C by fitting the heat transfer coefficient data measured in Newtonian and non-Newtonian system. Henzier [44] obtained the C value by fitting mass transfer coefficient data in non-Newtonian liquids in a bubble column tower reactor. Schumpe and Deckwer [31] proposed the value of C for

their studies in tower reactors for different diameter and different viscous liquids. The applicability of the Nishikawa et al. [43] and Henzier [44] correlation was questioned by a number of researchers [45-47]. In present study, C is taken as 2,800 m⁻¹ and effective viscosity was calculated by using Eq. (4).

2. Bubble Characteristics and Flow Regime

At very low air flow rate the bubbles of equal size are forms which demonstrate homogeneous flow region, but exist only for small range of flow rate variation. As the air flow rate increases, strong convective motion results, which brings the bubbles close together, allowing coalescence leading to the formation of larger bubbles. When the bubbles are sufficiently large and the concentration of SCMC solution is high enough, the bubbles appear to be cups at its lower end. Similar results are also observed by other researchers [48-50]. These large bubbles rise in the center of the column, carrying considerable amount of liquid and many small bubbles in their wake. Once the large bubbles reach the liquid surface, the small bubbles in the wake are entrained by the liquid downflow and are swept downward at the sides of the column. In almost the entire range of the study the flow pattern was heterogeneous as bubbles of varying size were produced. The flow pattern in the tapered bubble column consists of two zones, central zone and annular region. In the central zone most of the bubbles rise, whereas bubble breakup and downward flow occur in the annular region [19,49]. At high gas flow rate the bubbles burst at the surface causing ejection of fines of liquid droplets and inward dipping in the annular region (Fig. 2). Fig. 3 shows that the static pressure at 3rd or 4th manometer tapping suddenly increases and is due to re-entering of the gas-liquid flow from the annular region to the main central region.

It was observed that the bubbles expanded spherically at close to the orifice plate and evolved from a spherical shape to teardrop shape as they passed upwards. Initially, the surface tension dominated near the orifice plate and hence the bubbles were spherical and as they flowed upward the buoyancy played an important role in the growth of bubbles and also coalescence occurred. As bub-

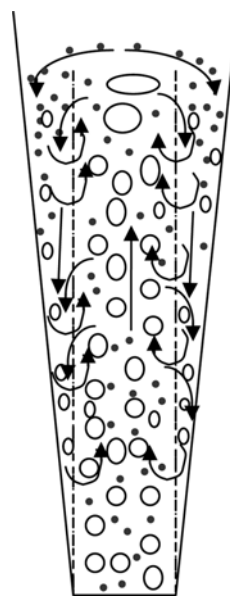


Fig. 2. Schematic diagram of the structure of a tapered bubble column.

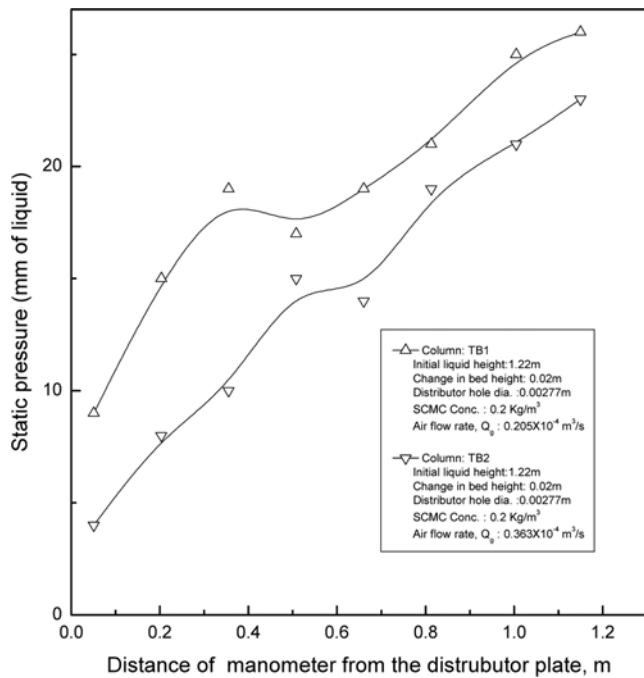


Fig. 3. Variation of static pressure with distance of manometer from the distributor plate.

bles move upward they tend to be elongated in shape and then in teardrop shape. As the bubbles move upward a non-Newtonian liquid is stretched because the reduction of viscosity takes place. In the shear thinning non-Newtonian liquid the apparent viscosity around the bubble decreases due to shear, hence bubbles can rise more easily. The viscosity of the liquid around the bubble varies; it depends on the shape of the bubble and shear-thinning property of the liquid, and the decrease of viscosity is more in the close vicinity of the bubble. A high viscosity region exists in the wake of these bubbles. The bubble rise velocity increases gradually due the strong shear-thinning effect. As shear-thinning effect becomes intensive, the bubble takes a more oblate shape with the front surface flatter than the rear part [50]. Similar observation is also reported by Anastasiou et al. [42] and Fransolet et al. [51]. Vélez-Cordero and Zenit [52] also identify the possibility of bubble cluster formation below the property group (N_{pl}) value of 1×10^{-3} .

3. Effect of SCMC Concentration on Hydrodynamic Parameters

Fig. 4 shows the variation of gas holdup with gas flow rate at different constant bed heights (1.12 m, 1.17 m, 1.22 m) for SCMC solutions. It is clear that the gas holdup increases with increasing gas flow rate at different constant bed height. As bed height increases, the gas holdup decreases with increasing gas flow rate. This is due to bubble coalescence in the column and its rise velocity increases. Fig. 5 shows the variation of gas holdup with gas flow rate at different SCMC concentrations. The gas holdup decreases with increasing SCMC concentration at constant gas flow rate. With increasing SCMC concentration effective viscosity increases; at higher SCMC concentration the dense medium will tend to reduce the bubble rise velocity and lead to longer residence time and also coalescence of the bubbles due to decrease of turbulence in the liquid phase, and it favors the formation of larger sized bubbles, which increases

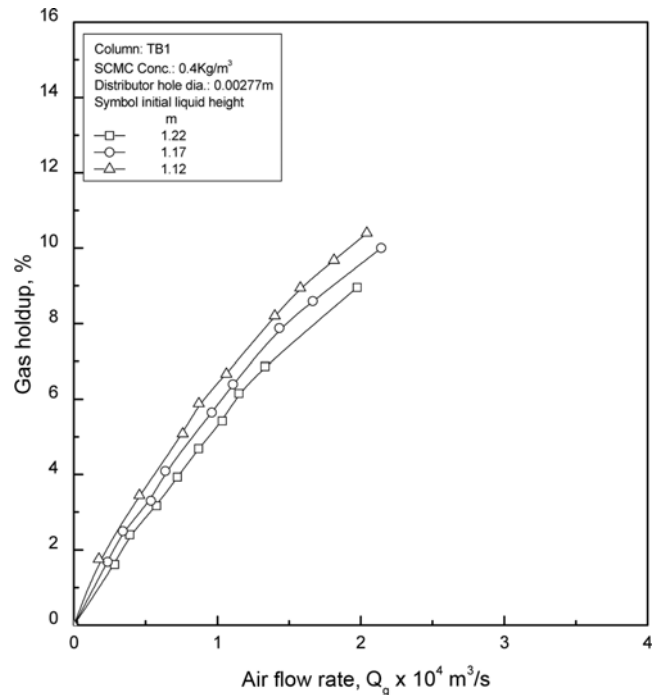


Fig. 4. Variation of gas holdup with gas flow rate at different clear liquid height.

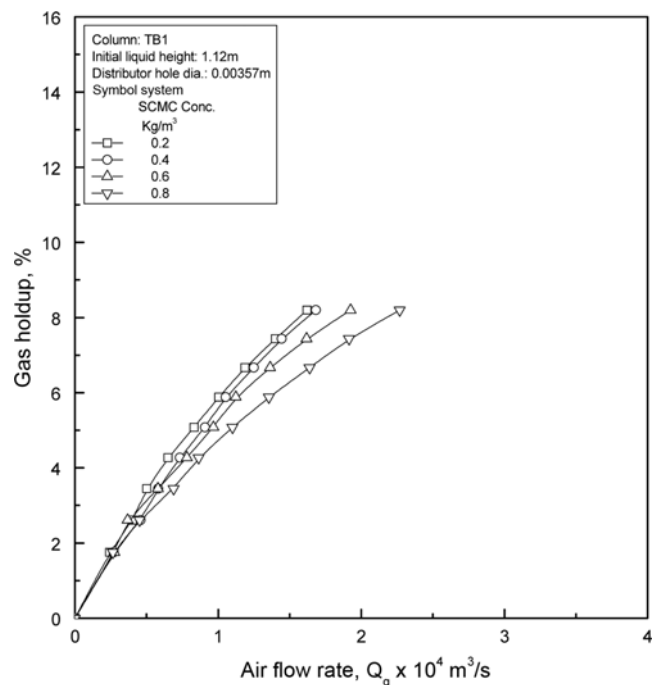


Fig. 5. Variation of gas holdup with gas flow rate at different SCMC solution concentration.

the bubble rise velocity. As SCMC concentration increases, the density of the solution increases; it leads to increase in buoyancy and hence bubble velocity. In these two opposite effects the latter is more predominant and is responsible for the low gas holdup at higher SCMC concentration. With the increase in SCMC concentration, the surface tension increases the expansion of bubble surface which is dif-

ficult and the bubble volume increases with coalescence only in the column. Similar results are also reported by other researchers [28,29,35,40,50].

4. Effect of Orifice Diameter

Bubble detachment volume gradually increases with the increase in orifice diameter, so the bubble size increases. Fig. 6 shows the variation of gas holdup with gas flow rate at different distributor

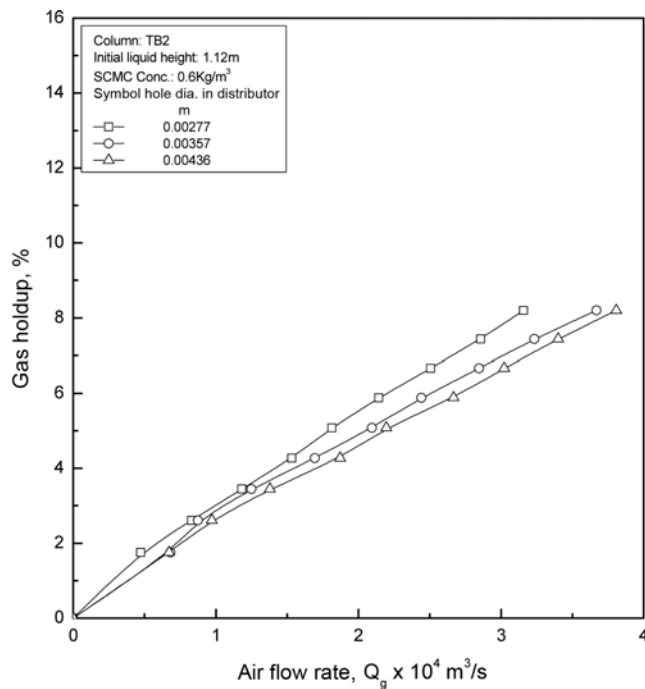


Fig. 6. Variation of gas holdup with gas flow rate at different hole diameter of the gas distributor.

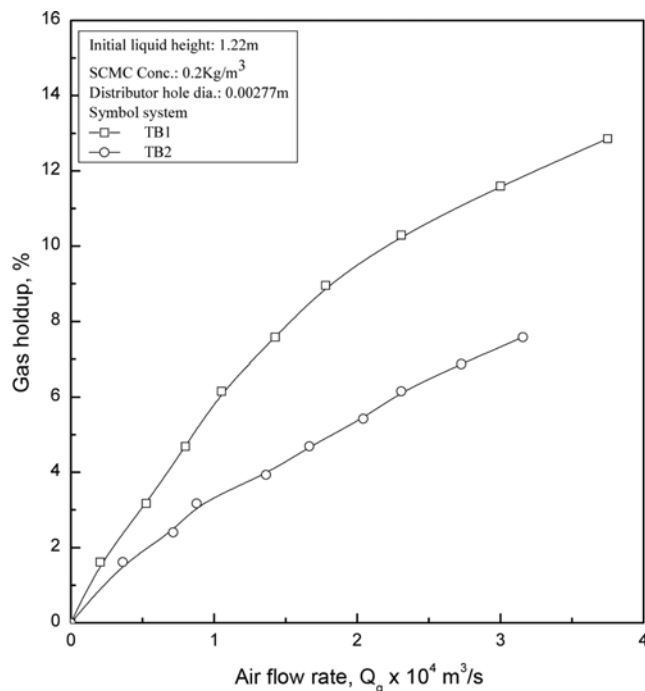


Fig. 7. Effect of the taper angle on holdup.

orifice diameters. It is clear that as the distributor orifice diameter increases, gas holdup decreases due to bigger sized bubble generation with higher bubble rise velocity.

5. Effect of Taper Angle

Fig. 7 shows the effect of taper angle on the gas holdup. It is clear that as the taper angle decreases the holdup increases. At lower taper angle back mixing is greater and at higher taper angle the liquid at near the wall in the upper half of the column remains unaffected, i.e., stagnant and hence holdup decreases. Increasing the taper angle the cross sectional area particularly in the upper zone increases, which minimizes the transition of flow pattern and also reduces the coalescence. In the case of a small taper angled bubble column the coalescence of bubbles is more, large sized bubble have higher rise velocity followed by small sized bubbles. Few of these small sized bubbles are recirculated through the annular region and are responsible for higher holdup. Whereas for higher taper angled bubble column the rate of recirculation is low due higher cross-sectional area in the upper zone and some portions close to the wall in the upper half of the column remain unaffected by the bubble.

6. Correlation for Holdup

Several empirical correlations for gas holdup are available in the literature. Schumpe and Deckwer [31] suggested the following correlation for their experiment in 0.102 m diameter bubble column using air-CMC solution in churn-turbulent flow regime:

$$\varepsilon_g = 0.725 U_g^{0.627}$$

This correlation does not take into account the physical properties of the gas-liquid system used. Godbole et al. [30] developed the following correlation for churn-turbulent flow regime:

$$\varepsilon_g = 0.225 U_g^{0.532} \mu_{eff}^{-0.146} \text{ for } U_g \geq 0.03 \text{ m/s and } 0.10 \text{ m} \leq D_c \leq 1.0 \text{ m} \quad (5)$$

Vatai and Tekic [53] reported an experimental investigation of gas holdup using non-Newtonian liquids and presented the following empirical correlation:

$$\varepsilon_g = 0.95 \left(\frac{U_g \mu_{eff}}{\sigma_1} \right)^{0.769} \left(\frac{\mu_{eff}^4 g}{\rho_l \sigma_1^3} \right)^{-0.17} \left(\frac{\rho_g}{\rho_l} \right)^{0.062} \left(\frac{\mu_g}{\mu_{eff}} \right)^{0.107}$$

for $D_c = 0.1 \text{ m}$; $H_o = 200 \text{ cm}$ (6)

Fransolet et al. [51] studied the effect of rheological behavior of the non-Newtonian pseudoplastic liquids on gas holdup and flow pattern in a bubble column reactor and developed the following equation:

$$\varepsilon_g = 0.26 U_g^{0.54} \mu_{eff}^{-0.147} \text{ for } D_c = 0.24 \text{ m, } U_g \leq 0.15 \text{ m/s} \quad (7)$$

Lakota [36] developed the following empirical correlation:

$$\varepsilon_g = 0.0524 U_g^{0.623} \mu_{eff}^{-0.0531} \text{ for } 0.018 \text{ m/s} \geq U_g \geq 0.252 \text{ m/s,}$$

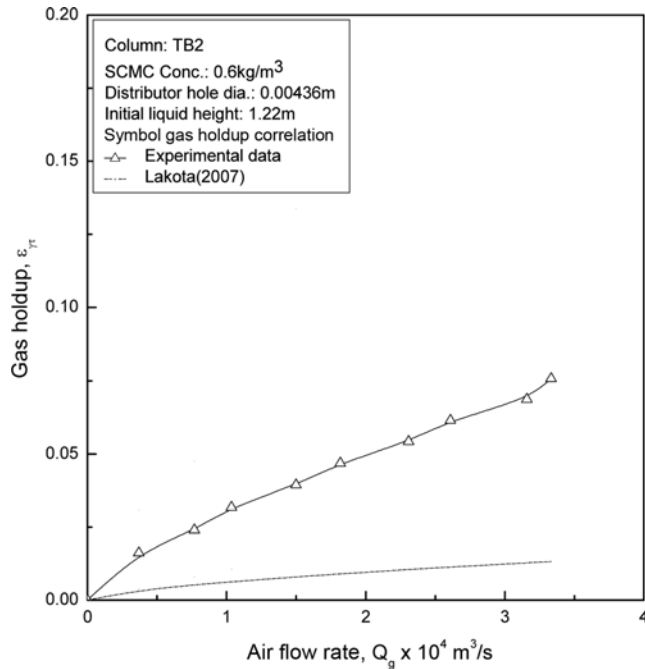
and $D_c = 2.62 \text{ m}$ and $H_o = 2.37 \text{ m}$ (8)

Except for Eq. (6) for all these correlations only viscosity terms have been introduced; the effects of other physical properties and system variables have not been considered, whereas in Eq. (6) the physical properties of the system are considered, not the system variables. The experimental gas holdup is compared with the above equations and Table 3 shows the relative error (RE) and absolute error (AE). The relative error and absolute error are defined as,

$$RE = \frac{1}{N} \sum_{i=1}^N \left| \frac{\varepsilon_{g\text{expt}} - \varepsilon_{g\text{cal}}}{\varepsilon_{g\text{expt}}} \right| \times 100 \quad (9)$$

Table 3. Comparison the holdup data with other correlation

Authors	RE (%)	AE
Godbole et al. [29]	82.106	0.016
Vatai and Tekic [54]	54.086	0.025
Fransolet et al. [52]	59.863	0.024
Lakota [34]	82.106	0.042
Eq. (13)	11.048	0.005

**Fig. 8. Comparison of gas holdup data with Lakota [34] correlation.**

$$AE = \frac{1}{N} \sum_{i=1}^N |(\varepsilon_{g,expt} - \varepsilon_{g,cal})| \quad (10)$$

Godbole et al. [30], Vatai and Tekic [53] and Fransolet et al. [51] correlations are valid for very high gas flow rate and chum-turbulent flow regime. Lakota [36] correlation is within our experimental range and Fig. 8 shows the comparison. It clearly shows that the performance of the taper column is more effective than the conventional cylindrical column.

As the above correlations are not correlated with the experimental data, hence, in the present case, a correlation has been developed by dimensional analysis to predict the gas holdup as a function of the physical properties, geometric and dynamic variables of the system. The parameters that affect the gas holdup for tapered bubble columns using non-Newtonian liquids are:

- (1) Physical properties of the gas and the liquid, namely, density ρ_g and ρ_l ; viscosity μ_g and μ_{eff} ; surface tension σ_l .
- (2) Gas flow rate of the gas Q_g .
- (3) Diameter of the column and distributor orifice diameter, namely, D_c and D_n .
- (4) Height of initial liquid in column, H_0 .
- (5) Taper angle (dimensionless), θ .
- (6) Other parameter like acceleration due to gravity, g .

The gas holdup may be written as a function of all these variables as,

$$\varepsilon_g = F(Q_g, \mu_g, \rho_g, \rho_l, \mu_{eff}, \sigma_l, H_0, D_c, D_n, \theta, g) \quad (11)$$

The diameter of the column is calculated by calculating the equivalent diameter of the base and at the gas-liquid interface, then by calculating the log mean diameter for the column, D_c . Hence, for each gas flow rate the column diameter, D_c , varies according to the height of the gas-liquid interface.

Applying Buckingham's π -theorem of dimensional analysis and also combining some of these group yields the following functional relationship:

$$\varepsilon_g = F\left(\text{Re}_g, N_{pl}, \frac{H_0}{D_c}, \frac{D_n}{D_c}, \theta\right) \quad (12)$$

On the basis of Eq. (12) the multiple linear regression analysis of the experimental data yielded the following correlation:

$$\varepsilon_g = 3.857 \times 10^{-4} \text{Re}_g^{0.743 \pm 0.017} N_{pl}^{-0.009 \pm 0.003} \left(\frac{H_0}{D_c}\right)^{-0.565 \pm 0.038} \left(\frac{D_n}{D_c}\right)^{0.149 \pm 0.063} \theta^{-0.706 \pm 0.028} \quad (13)$$

for

$$6.0615 \leq \text{Re}_g \leq 417.91$$

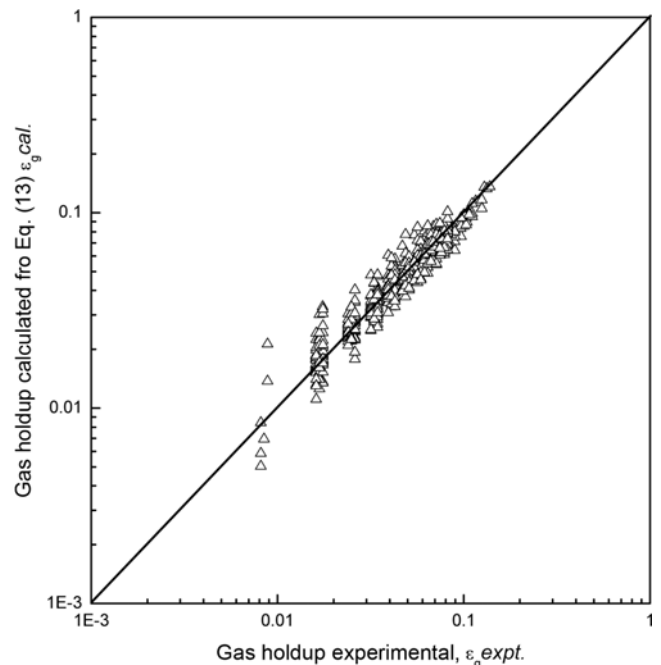
$$8.17 \times 10^{-8} \leq N_{pl} \leq 3.10 \times 10^{-2}$$

$$16.91 \leq \left(\frac{H_0}{D_c}\right) \leq 20.13$$

$$0.03914 \leq \left(\frac{D_n}{D_c}\right) \leq 0.07275$$

$$0.0077 \leq \theta \leq 0.015$$

where, the liquid property group, $N_{pl} = \mu_{eff}^4 g / \rho_l \sigma_l^3$, signifies some complex balance between viscous, surface tension and gravitational

**Fig. 9. Correlation plot of gas holdup.**

force. The values of the prediction by Eq. (13) have been plotted against the experimental values as shown in Fig. 9. The variance of the estimate and correlation coefficient of the above equation are 0.02191 and 0.9616, respectively, for a t value of 1.98 for 641 degrees of freedom at 0.05 probability levels and 95% confidence range [54].

CONCLUSIONS

Experiments have been carried out to measure the gas holdup for two different taper bubble columns using non-Newtonian pseudo-plastic liquids. The gas holdup increases with decrease the bed height and distributor orifice diameter. The gas holdup decreases with increasing the pseudoplasticity of SCMC solution. An empirical correlation, Eq. (13), has been developed to calculate the gas holdup as a function of various measurable parameters.

NOMENCLATURE

D_c	: diameter of column (log mean) [m]
D_n	: distributor orifice diameter [m]
g	: acceleration due to gravity [m/s^2]
H_0	: initial liquid height in column [m]
K	: consistency index [Ns''/m^2]
n	: flow behaviour index (dimensionless)
Q_g	: gas flow rate [m^3/s]
U	: superficial velocity [m/s]
V	: volume of the dispersion [m^3]
V_o	: volume of the clear liquid [m^3]
N_{pl}	: liquid property group, $N_{pl} = \mu_{eff}^4 g / \rho_l \sigma_l^3$ (dimensionless)
Re_g	: Reynolds number of gas, $(U_g D_c \rho_g / \mu_g)$ (dimensionless)
TB1	: smaller tapered bubble column
TB2	: larger tapered bubble column

Greek Letters

α	: taper angle, deg.
ρ	: density [kg/m^3]
ε_g	: gas holdup, dimensionless
σ_l	: surface tension [N/m]
θ	: taper angle [rad]
μ_{eff}	: effective viscosity [$Pa \cdot s$]
τ	: shear stress [N/m^2]
$\dot{\gamma}$: shear rate [s^{-1}]

Subscripts

g	: gas
l	: liquid
eff	: effective

REFERENCES

- J. B. Joshi, *Chem. Eng. Sci.*, **56**, 5893 (2001).
- B. N. Thorat, K. Kataria, A. V. Kulkarni and J. B. Joshi, *Ind. Eng. Chem. Res.*, **40**, 3675 (2001).
- A. Mouza, G. K. Dalakoglou and S. V. Paras, *Chem. Eng. Sci.*, **60**, 1456 (2005).
- A. A. Kulkarni and J. B. Joshi, *Ind. Eng. Chem. Res.*, **44**, 5873 (2005).
- W. D. Deckwer, *Int. Chem. Eng.*, **19**, 21 (1979).
- N. Kantarci, F. Borak and K. O. Ulgen, *Proc. Biochem.*, **40**, 2263 (2005).
- Y. T. Shah, B. G. Kelkar, S. P. Godbole and W. D. Deckwer, *AIChE J.*, **28**, 353 (1982).
- D. A. Hines, Proc. 1st Eur. Congr. Biotechn, CH-Interlaken, Sep. 1978, Dechema Monographs, 82, 55, Verlag Chemie, Weinheim (1978).
- J. B. Joshi and M. M. Sharma, *Trans. Inst. Chem. Engrs.*, **54**, 42 (1976).
- P. Herbrechtsmeier and R. Steiner, *Chem. Ing. Technol.*, **50**, 944 (1978).
- K. Schugerl, J. Lucke, I. Lehmann and F. Wagner, *Adv. Biochem. Eng.*, **8**, 63 (1978).
- G. Kundu, D. Mukherjee and A. K. Mitra, *Int. J. Multiphase Flow*, **21**, 893 (1995).
- A. Mandal, G. Kundu and D. Mukherjee, *Chem. Eng. Sci.*, **59**, 3807 (2004).
- C. D. Scott and C. W. Hancher, *Biotechnol. Bioeng.*, **18**, 1393 (1976).
- W. W. Pitt, C. W. Hancher and B. D. Patton, *Nucl. Chem. Waste Manage.*, **2**, 57 (1981).
- J. S. Huang, J. L. Yan and C. S. Wu, *J. Chem. Technol. Biotechnol.*, **75**(4), 269 (2000).
- D. D. Lee, C. D. Scot and C. W. Hancher, *J. (Water Pollution Control Federation)*, **51**(5), 974 (1979).
- K. Zhang, Y. Zhao and B. Zhang, *Int. J. Chem. Rea. Eng.*, **1**, Note S3 (2003).
- S. Sen, *Studies on hydrodynamics of tapered bubble column*, M. Tech Thesis, University of Calcutta, Kolkata (2003).
- P. S. Mandal, B. Basak and S. K. Das, *Proc. Int. Conf. Chem. Eng.*, 29-30 Dec. 2003, Bangladesh, 166 (2003).
- J. J. Chen, M. Jamialahmadi and S. M. Li, *Chem. Eng. Res. Des.*, **67**, 203 (1989).
- D. C. Sau, S. Mohanty and K. C. Biswal, *Chem. Eng. J.*, **132**(1-3), 151 (2007).
- T. M. Gernon, M. A. Gilbertson and R. S. J. Sparks, *Particle segregation in tapered fluidized beds*, 13th Int. Conf Fluidization - New Paradigm in Fluidization Engineering, Available at http://dc.confintl.org/fluidization_xiii/91 dt. 10.3.2013.
- Y. F. Shi, Y. s. Yu and L. T. Fan, *Ind. Engg. Chem. Fundam.*, **23**, 484 (1984).
- T. M. Gernon and M. A. Gilbertson, *Powder Technol.*, **231**, 88 (2012).
- R. Parthiban, *Songklanakarinn J. Sci. Technol.*, **33**(5), 539 (2011).
- D. Chakraborty, M. Guha and P. K. Banerjee, *Chem. Eng. Commun.*, **196**(9), 1102 (2009).
- R. P. Chhabra, *Bubbles, drops, and particles in non-newtonian fluids*, CRC, Taylor & Francis (2007).
- R. P. Chhabra, *Hydrodynamics of bubbles and drops in rheologically complex fluids*, *Encyclopedia of Fluid Mechanics 7*; Gulf Publishing Co., London, 253 (1988).
- S. P. Godbole, M. F. Honath and Y. T. Shah, *Chem. Eng. Commun.*, **16**, 199 (1982).
- A. Schumpe and W. D. Deckwer, *Ind. Eng. Chem. Process. Des. Dev.*, **21**, 706 (1982).

32. A. Schumpe and W. D. Deckwer, *Bioprocess. Eng.*, **2**, 79 (1987).
33. S. K. Chandrakar, *Gas dispersion in non-Newtonian liquid-jet ejectors and two phase co-current vertical upflow*, PhD Thesis IIT Kharagpur (1985).
34. M. W. Haque, K. D. P. Nigam and J. B. Joshi, *Chem. Eng. Sci.*, **41**, 2321 (1986).
35. H. J. Li, *Chem. Eng. Sci.*, **54**, 2247 (1999).
36. A. Lakota, *Acta. Chim. Slov.*, **54**, 678 (2007).
37. A. K. Pradhan, R. K. Parichha and P. De, *Can. J. Chem. Eng.*, **71**, 468 (1993).
38. S. K. Das, M. N. Biswas and A. K. Mitra, *Can. J. Chem. Eng.*, **70**, 431 (1992).
39. A. Mandal, G. Kundu and D. Mukherjee, *Chem. Eng. and Proc.*, **42**, 777 (2003).
40. S. K. Chandarkar, S. K. Das and M. N. Biswas, *Pressure drop in gas dispersion in non-Newtonian liquid jet ejector system*, *Int. Conf. Adv. Mechanical and Building Science in the 3rd Millennium*, 14-16 Dec., VIT University, TN (2009).
41. M. W. Haque, K. D. P. Nigam, K. Viswanathan and J. B. Joshi, *Ind. Eng. Chem. Res.*, **26**, 86 (1987).
42. A. D. Anastasiou, A. D. Passos and A. A. Mouza, *Chem. Eng. Sci.*, **98**(19), 331 (2013).
43. M. Nishikawa, H. Kato and K. Hashimoto, *Ind. Eng. Chem. Process. Des. Dev.*, **16**, 133 (1977).
44. H.-J. Henzler, *Chem. Ing. Technol.*, **56**, 422 (1984).
45. D. G. Allen and C. W. Robinson, *Biotechnol. Bioeng.*, **38**, 212 (1991).
46. Y. Chisti and M. Moo-Young, *Biotechnol. Bioeng.*, **34**, 1391 (1989).
47. Y. Kawase and T. Kamagai, *Bioproc. Eng.*, **7**, 25 (1991).
48. W. A. Al-Masry, *Biotechnol. Bioeng.*, **62**, 494 (1999).
49. O. Hassager, *Nature*, **279**, 402 (1979).
50. C. Málaga and J. M. Rallison, *J. Non-Newtonian Fluid Mech.*, **141**, 59 (2007).
51. E. Fransolet, M. Crine, P. Marchot and D. Toye, *Chem. Eng. Sci.*, **60**, 6118 (2005).
52. J. R. Vélez-Cordero and R. Zenit, *J. Non-Newtonian Fluid Mech.*, **166**, 32 (2011).
53. G. Y. Vatai and M. N. Tekic, *Chem. Eng. Sci.*, **42**(1), 166 (1987).
54. V. Volk, *Applied statistics of engineers*, McGraw-Hill, New York, 345 (1958).